Geometry of approximant structures in quasicrystals

1995 J. Phys.: Condens. Matter 7 9101

(http://iopscience.iop.org/0953-8984/7/48/004)

J. Phys.: Condens. Matter 7 (1995) 9101–9125. Printed in the UK

Geometry of approximant structures in quasicrystals

D Gratias†, A Katz‡ and M Quiquandon†
† CECM/CNRS, 15 rue G. Urbain, F-94407 Vitry-Cedex, France
‡ CPT, Ecole Polytechnique, F-91128 Palaiseau-Cedex, France

Received 2 June 1995

Abstract. We present a specific geometric description of the approximant phases in quasicrystals using a classification based on symmetry arguments. We derive the 'shear' technique as a special case of this description and discuss the cases of periodic approximants.

Observing that all presently known approximant phases have high point symmetry, we make the conjecture that these phases are stabilized by a 'lock-in'-like phenomenon based on maximizing the number of easy atom flips.

1. Introduction

All presently known stable quasicrystals are crucially sensitive to chemical composition. Their equilibrium phase diagrams show in the vicinity of their stability region several closely related complex intermetallic phases called 'approximant structures'. Most of these phases have been recognized as 3D periodic structures with large unit cells. They exhibit diffraction patterns very similar in intensity and peak positions to those of the parent quasicrystalline phase (see, for instance, [1]). Their physical properties are so close to those of the parent quasicrystal that it is often impossible to experimentally distinguish between approximants and quasicrystals but by high resolution diffraction experiments. Electron microscopy images strongly suggest that the local packing of these approximants resembles closely that of the quasicrystal, the 'quasicrystalline' effect being observed only at large distances.

From the geometric point of view, the similarities between these phases have a straightforward explanation: quasicrystals can be considered as 'interpolation' between crystalline phases or as the limit of sequences of crystals with increasing unit cells exactly as irrational numbers are limits of sequences of rational numbers.

Incommensurate and quasicrystalline phases are best described in the framework of n-dimensional crystallography [2–5]. In that scheme, atoms are represented by periodically spaced $(n-3)$-dimensional manifolds transverse to the physical 3D space. The real incommensurate or quasicrystalline phase is obtained by simply intersecting this N-dimensional object by the 3D physical space. Approximants are thus generated by choosing a cut space in a 'direction' close to the original one used to generate the parent quasicrystal [6–8]: it is this 'direction' which characterizes the approximant and which must be determined from the experimental data. This technique has been implemented in the framework of the strip (or cut-and-project) method [9–13] by Duneau [14] who introduced an 'oblique' projection of the lattice nodes (inside the strip) onto the physical space and has shown to be very efficient as exemplified by Duneau and co-workers [15] in the case of the octagonal tiling.

Ishii [16–18] calculated the possible cut 'directions' by defining n-dimensional rotation matrices as functions of the point symmetry group of the approximant in an exhaustive

0953-8984/95/489101+25$19.50

study based on irreducible representations in group theory. This very general approach is extremely useful for determining which kind of irreducible representations should be considered when a symmetry breaking of the quasicrystal occurs. A very detailed and complete analysis of these rotation matrices is given by Baake [19] and Kramer [20] and applied to defining approximants.

An earlier approach was proposed several years ago by Jaric and Mohanty [8] in a slightly different context, based on the idea that an approximant phase can be looked upon as the result of a homogeneous 'shear' of the underlying hyperspace lattice, which we denote by Λ. The essence of the method consists in assuming that certain rational lattice directions of Λ can be aligned with the parallel space denoted by $E_{\parallel}$, under a shear transformation. Obviously, as for any geometric analysis, no physical scheme of the elementary mechanisms should be directly deduced from this shear picture, but it shows explicitly which atoms should move to lead to the approximant phase and predicts the geometric relationships which should be observed between the two phases. After the initial work of Jaric and Mohanty [8], the 'shear' method was implemented and used in real cases by Yamamoto and Ishihara [21, 22], Jaric and Qiu [23] and Janssen [24]. This method turned out indeed to be extremely efficient and accurate for predicting the lattice parameters of the possible periodic approximants. As well as its simplicity, the method is very economical for calculating the diffraction patterns of the approximants.

Our present purpose is to construct a simple specific formulation that can be directly used by diffractionists for analysing *real* cases. Real quasicrystals and tilings share some basic properties which are due to one fundamental feature: they both are described with 'flat' atomic surfaces [25]. Therefore, real quasicrystals exhibit only a *finite* number of different atomic environments (up to a given distance) out of which specific atomic clusters can be extracted to exemplify the structure. Also, the atomic positions of real quasicrytals can be viewed (generally, in several ways) as a quasiperiodic tiling generated with a finite number of prototiles. Although strip(s) and cut are equivalent for describing quasicrystals with flat atomic surfaces, we choose the cut method because it is the most natural description of quasiperiodic objects in the sense that it is the closest to the very definition of quasiperiodicity, the simplest for discussing symmetry arguments in the high dimension space and the easiest for linking quasicrystals to incommensurate phases.

As well as this general goal, we will emphasize the special case of the 'periodic' approximants because of their practical importance (see, for instance, [1, 26–30]). Periodic approximants, by their very definition, do not require the high dimension space formalism for their description. However, this formalism is useful: it allows us to define in a unified way whole families of approximant periodic structures corresponding to a single direction of the cut, for which each family is parametrized by a discrete version of the 'phason' degree of freedom associated with translations in the perpendicular space. As we shall see, it is possible to single out special approximants characterized by the perpendicular space position of the associated cuts. We wish to discuss in some detail this 'lock-in' process because of its importance in the geometric description of quasicrystal/crystal phase transformations.

The paper is organized into three main sections. In the first section, we present the geometric method we use to construct quasiperiodic structures in a way suitable to easily separate the effect of the distortion of the atomic surfaces (the so-called 'phonon' field) from the effect of tilting the direction of the cut space (the so-called 'phason' field); the second section introduces symmetry arguments for constructing a classification scheme of the various possible approximants in connection with the shear method; the third section discusses the method for the specific case of periodic approximant phases.

2. Geometric characterization of approximant phases

We designate by approximant, a (quasiperiodic or periodic) structure with a diffraction pattern 'close' to the diffraction pattern of a given high symmetry quasicrystal, from both points of view of peak locations and intensities. The high symmetry quasicrystal will be called hereafter the 'parent quasicrystal'. Under these definitions, an approximant phase is not necessarily periodic in one or several directions.

2.1. Algorithm of construction

As already mentioned, we start from the original cut method as introduced for quasicrystals by Bak [4, 5] after the pioneer work of de Wolff [2] and Janner and Janssen [3].

For our specific purpose of using 'flat' atomic surfaces, the simplest cut algorithm consists in copying in $\mathbb{R}^n$ a prototypic 'atomic surface' σ—which is a bounded volume of a $(n - d_\parallel)$-dimensional vector subspace noted $E_\perp$—at each node of a lattice Λ in $\mathbb{R}^n$ and selecting their intersection with a cut space, say $E_\parallel$, of dimension $d_\parallel$ (the physical space) perpendicular to the atomic surfaces and irrationally oriented with respect to Λ. We only need a slight generalization of this initial algorithm to generate approximant phases. (i) The atomic surfaces σ, which are still supposed to be flat, are no longer necessarily parallel to $E_\perp$; we denote by E_σ the space carrier of the atomic surfaces. (ii) We introduce an intermediate cut space E_c, which will be used to collect the points defining the atomic positions in the final structure, that is no longer necessarily parallel to the physical space $E_\parallel$. We designate by $d_\perp = n - d_\parallel$ the dimension of the perpendicular spaces $E_\perp$ and $E_c^\perp$. We assume that E_σ and $E_\perp$ have the same dimension and that E_σ and E_c are properly oriented with respect to $E_\parallel$ in the sense that E_σ is transverse to E_c which, in turn, projects one-to-one onto $E_\parallel$ along $E_\perp$.

To generate the structure, we proceed in the following way. (i) We copy the prototypic atomic surface σ at each lattice node (the method generalizes trivially to several atomic surfaces per unit cell). (ii) We then take the intersection of these surfaces with E_c. (iii) Finally we project the collected points onto $E_\parallel$ along $E_\perp$ (see figure 1). This technique of using both a cut *and* a projection is, to some extent, arbitrary but it has the advantage of both separating the displacement field from the flip field (see next subsection) and leading to a simple formulation for the Fourier transform.

We can compute the mass density μ associated with the final structure. For that purpose, we introduce the following notations. Λ is the n-D lattice, bearing one Dirac δ at each vertex; $\eta = \eta_\sigma \otimes \delta_{0 \in E_\sigma^\perp}$ is the measure carried by the atomic surface σ: it is the product of the characteristic function η_σ within E_σ (η_σ takes value 1 inside the atomic surface and 0 outside) by a Dirac δ located at the origin of $E_\sigma^\perp$; $\mathrm{d}x_{E_j} = 1_{E_j} \otimes \delta_{0 \in E_j^\perp}$ is the Lebesgue measure carried by the subspace E_j.

Now, we follow the geometric construction. (i) The prototypic atomic surface is copied at each lattice node of Λ; this is obtained by the convolution product $\Lambda * \eta$. (ii) Next, this set is cut by E_c; this leads to $(\Lambda * \eta) \cdot \mathrm{d}x_{E_c}$ (at that stage, we obtain a set of points in E_c). (iii) Finally, we project this set of points in E_c onto $E_\parallel$: we copy $E_\perp$ at each point of this set by the convolution $((\Lambda * \eta) \cdot \mathrm{d}x_{E_c}) * \mathrm{d}x_{E_\perp}$ and take the intersection with $E_\parallel$.

All together, we obtain

$$\mu = (((\Lambda * \eta) \cdot \mathrm{d}x_{E_c}) * \mathrm{d}x_{E_\perp}) \cdot \mathrm{d}x_{E_\parallel}. \tag{1}$$

The parent quasicrystal is defined by $E_\sigma = E_\perp$ and $E_c = E_\parallel$.

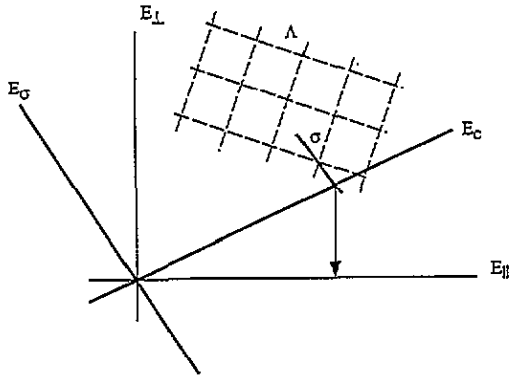

Figure 1. The cut method extended to take into account both perpendicular and parallel displacements: the subspace E_σ carrying the atomic surfaces is no longer parallel to $E_\perp$ and the subspace E_c collecting the intersection points is no longer parallel to $E_\parallel$ neither perpendicular to E_σ.

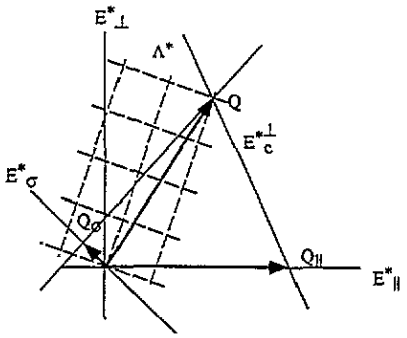

Figure 2. Construction of the Fourier spectrum obtained by the extended cut method: reciprocal vectors Q of Λ^* are projected onto $E_\parallel^*$ along $E_c^{\perp *}$. The amplitude of the diffracted beam is calculated using the orthogonal projection of Q onto E_σ^*.

The Fourier transform $\widehat{\mu}$ is obtained by performing the following formal transformations:

$$\begin{aligned}
&\mu \to \widehat{\mu}\\
&\eta \to \widehat{\eta}\\
&(\ldots)\cdot(\ldots) \to (\widehat{\ldots}) * (\widehat{\ldots})\\
&(\ldots)*(\ldots) \to (\widehat{\ldots})\cdot(\widehat{\ldots})\\
&\mathrm{d}x_E \to \delta_{0\in E^*}\\
&\delta_{0\in E} \to \mathrm{d}x_{E^*}\\
&(\ldots)\otimes(\ldots) \to (\widehat{\ldots})\otimes(\widehat{\ldots})
\end{aligned} \tag{2}$$

where, as usual, star superscripts designate the various reciprocal spaces. Using these rules and noting that $\widehat{\Lambda} = \Lambda^*$, $\widehat{\eta} = \widehat{\eta_\sigma} \otimes \mathrm{d}x_{E_\sigma^{\perp *}}$, and $\widehat{\mathrm{d}x_{E_j}} = \mathrm{d}x_{E_j^{\perp *}}$, we obtain the Fourier transform $\widehat{\mu}$ of the mass density (1):

$$\widehat{\mu} = (((\Lambda^* \cdot (\widehat{\eta_\sigma} \otimes \mathrm{d}x_{E_\sigma^{\perp *}})) * \mathrm{d}x_{E_c^{\perp *}}) \cdot \mathrm{d}x_{E_\parallel^*}) * \mathrm{d}x_{E_\perp^*}. \tag{3}$$

The geometric interpretation of equation (3), shown in figure 2, is as follows. (i) We first take the value of the Fourier transform $\widehat{\eta}$ of the characteristic function η_σ using as the argument the projections of the nodes of Λ^* along $E_\sigma^{\perp *}$ onto $E_\sigma{}^*$. (ii) Then, to obtain the carrier of the Fourier transform, we make the oblique projection of Λ^* along $E_c^{\perp *}$ onto $E_\parallel^*$. (iii) The final Fourier amplitude is obtained by multiplying the previous value of $\widehat{\eta}$ by a correction term due to the fact that $\mathrm{d}x_{E_c^{\perp *}}$ is not perpendicular to $\mathrm{d}x_{E_\parallel^*}$.

The last convolution with $\mathrm{d}x_{E_\perp^*}$ in (3) is here for consistency; it simply means that the Fourier transformation of a $d_\parallel$-dimensional object in an n-dimensional space has an $(n - d_\parallel)$-dimensional trivial extension in the complementary space. The Fourier transform actually observed in reciprocal space is the restriction in $E_\parallel^*$ of (3), i.e. the whole expression truncated at the level of the last convolution with $E_\perp^*$.

This symbolic notation is very powerful in showing the main geometric features of the Fourier transform: (i) the locations of the peaks in the diffraction pattern depend only on the

direction of E_c, irrespective of the direction of E_σ; (ii) the intensities of the peaks depend on both E_σ and E_c.

Hence, the experimental determination of the direction of E_c only requires the determination of the *locations* of the diffraction peaks with respect to those of the parent quasicrystal irrespective of their intensities.

On the other hand, the determination of the direction of E_σ requires measuring *both* the locations and the integrated intensities of the diffraction peaks (or high resolution imaging if the atomic displacements are large enough to be observed). This is very similar to standard structure determination in usual crystals: the space group identification (irrespective of a possible inversion symmetry) is achieved by purely geometric analysis of the diffraction patterns (point symmetry and possible systematic extinction of certain reflections); the relative locations of the atoms are determined by a further quantitative analysis of the integrated intensities of the peaks.

2.2. *'Shift' and 'flip' fields*

A rational orientation of E_c with respect to Λ generates a periodic structure (1D, 2D or 3D): the resulting structure is a periodic collection of atomic clusters where atoms are in general at locations which are incommensurate with the lattice parameters.

Modifying the direction of the cut space E_c with respect to $E_\parallel$, while keeping E_σ constant, results in a reshuffling of the atomic local configurations. This corresponds to the so-called 'linear phason' field which we prefer to designate here as the flip field because, in the present context, we do not refer to dynamical modes. It describes the set of collective flips of atoms which are needed to transform the given quasicrystal into the approximant structure. We notice that this description is only a geometric approach and does not refer to a specific physical mechanism in the transition. Indeed, although this geometric picture would suggest martensitic instabilities (see [8]) for characterizing these transitions from quasicrystal to approximants, all presently available experimental results clearly support long distance atomic diffusion processes.

On the other hand, a rational orientation of E_σ leads to a quasiperiodic atomic selection of sites all belonging to a host (periodic) lattice: a tilt of E_σ with respect to $E_\perp$ alters the relative distances between the atoms with no change in the topology of the local environment. This corresponds to the so-called 'phonon' field which, again, we prefer to call the 'shift' field since, here too, it refers to static distortions with no direct connection with lattice dynamics. These displacements of the atomic positions are linear functions of the coordinates of the lattice nodes of Λ in $E_c^\perp$.

A prescription must be given to define the distortions of the atomic surfaces of real quasicrystals under a shift or a flip field.

The very possibility for defining these distortions relies on the so-called 'closeness property' of the atomic surfaces. Let us recall briefly the basic ideas of this hypothesis [31, 32]. Consider the cut construction of any (quasi)periodic structure, and shift the cut: it is natural to require that, each time the cut leaves an atomic surface by crossing its boundary, then it enters a neighbouring atomic surface, in such a way that no atom appears nor disappears upon such a shift, but simply jumps from one position to a neighbouring one. For canonical tilings, this jump defines the local reconstruction known as a 'flip', and the closeness condition merely requires the same kind of local reconstruction to occur in any realistic description of quasicrystals. It should be emphasized that this closeness property is a basic feature of all the structures considered in this paper. In fact, this property is necessary for the comparison between structures differing through a tilt of E_c and/or E_σ to make sense.

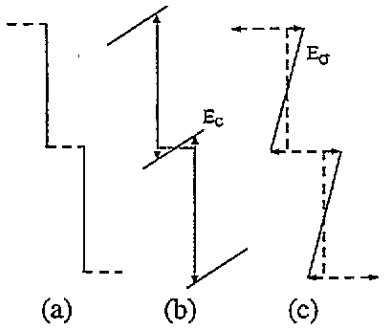

Figure 3. Deformation of the atomic surfaces of the parent quasicrystal (*a*); under a flip field (*b*) and a shift field (*c*).

From a geometric point of view, this constraint means that it is possible to add to the original atomic surfaces, new pieces linking together the boundaries of these atomic surfaces (and which may be loosely thought of as the possible trajectories of jumping atoms), in such a way that there are no longer boundaries for the set of 'completed' atomic surfaces. Moreover, the new pieces must be non-transversal to the cut so that they do not intersect it each time it is in generic position and nothing is changed in the structure.

Now, the prescription for defining the distortions of the atomic surfaces under a shift or a flip field becomes obvious: we impose that the connections between neighbouring atomic surfaces remain the same, or in other words, that the topology of the completed atomic surface is left unchanged, as sketched in figure 3.

The procedure is defined for a continuous set of directions of $\boldsymbol{E}_c$ (or $\boldsymbol{E}_\sigma$) including those corresponding to periodic structures in $\boldsymbol{E}_\parallel$. It is equivalent, in the strip method, to defining the acceptance window as the projection of the hyperlattice unit cell onto $\boldsymbol{E}_c^\perp$ for the generation of tilings called canonical tilings. Shift and flip fields with adequate distortions of the atomic surfaces are shown in figure 4.

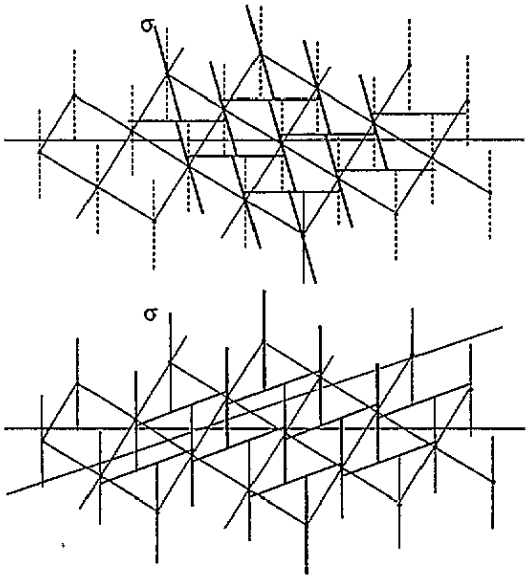

Figure 4. Atomic surface deformations from the parent quasicrystal (in broken lines on the top figure) under: (top) a shift field, and (bottom) a flip field. In both cases, the overall topology of the atomic surfaces has been kept invariant.

Examples of resulting structures are exemplified in figure 5 for the case of the canonical octagonal tiling for some directions of $\boldsymbol{E}_c$ and $\boldsymbol{E}_\sigma$.

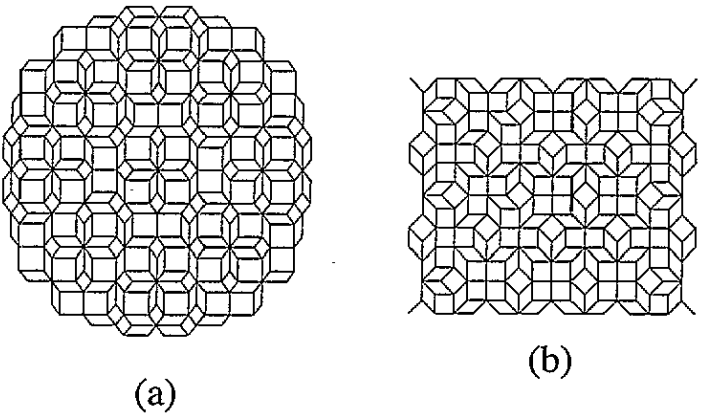

Figure 5. Examples in the octagonal tiling: (*a*) through a pure shift field the tiles are distorted but they connect as in the octagonal tiling; (*b*) through a pure flip field the tiles have same shape but they connect differently than in the octagonal tiling.

3. Projectors and symmetries

Our strategy consists in classifying the subspaces E_σ, E_c, $E_\perp$ and $E_\parallel$ introduced in the previous section with respect to their symmetry properties: the set of all subspaces with the same dimension that are invariant through the action of a given point group, say $\mathcal{H}$, subgroup of the point group $\mathcal{G}$ of the parent quasicrystal defines the *$\mathcal{H}$-stratum* in $\mathcal{G}$.

3.1. Symmetry strata

Projection operators are linear maps that project the Euclidean superspace, $\mathbb{R}^n$ onto the subspaces of interest (which we will denote by E_α, where α, a generic symbol, stands for any of the symbols σ, c, $\perp$, $\parallel$, ...). They can be represented by $n \times n$ real matrices π_α of rank d_α such that

$$\pi_\alpha^2 = \pi_\alpha \tag{4}$$

and

$$E_\alpha = \{\xi \in \mathbb{R}^n; \quad \pi_\alpha \xi = \xi\}. \tag{5}$$

Equations (4) and (5) do not determine the projector π_α completely from its image E_α, since the direction along which the projection is made is still free. In order to fix this relation, we use orthogonal projections, i.e. in this context, symmetric matrices:

$${}^t\pi_\alpha = \pi_\alpha. \tag{6}$$

On the other hand, it is immediate from equations (4) and (5) that $I - \pi_\alpha$ is a projector which verifies $(I - \pi_\alpha) \cdot \pi_\alpha = 0$, so that it projects along E_α onto the subspace $E_\alpha^\perp$ orthogonal to E_α. Observe that the dimension d_α of E_α is equal to the trace of the matrix π_α.

Now, if we have the expression of π_α as an $n \times n$ symmetric matrix with real entries, it is easy to build an orthonormal basis of E_α, $\mathcal{B}_\alpha = \{e_\alpha^j;\ j = 1, 2, 3, \ldots, d_\alpha\}$ by choosing

any d_α columns of the π_α matrix and performing a standard Schmidt orthogonalization on this set.

Let $g \in \mathcal{H}$ be a symmetry operation of the hyperlattice Λ, in $\mathbb{R}^n$. A subspace $\boldsymbol{E}$ is invariant through g if and only if g *commutes* with the projector π associated with $\boldsymbol{E}$.

In fact, for every $\xi \in \mathbb{R}^n$ we have always $\pi g\xi \in \boldsymbol{E}$, and if g preserves $\boldsymbol{E}$, then $g\pi\xi \in \boldsymbol{E}$. Thus, we have to verify $\pi g - g\pi = 0$ on $\boldsymbol{E}$. But on $\boldsymbol{E}$, π is the identity and the result follows.

Conversely, if $\pi g - g\pi = 0$, let us take $\xi \in \boldsymbol{E}$. Then we get $g\pi\xi = g\xi = \pi g\xi \in \boldsymbol{E}$, which shows that g preserves $\boldsymbol{E}$. Therefore a subspace $\boldsymbol{E}$ is invariant through a certain point symmetry group $\mathcal{H}$ if and only if its projector commutes with the considered group, i.e. if the projector commutes with the generators of the group. The set of all projectors with trace d which commute with $\mathcal{H}$ corresponds to a family of subspaces of dimension d which are invariant through the action of $\mathcal{H}$. This family is referred to as the *stratum* $\boldsymbol{E}_d^{\mathcal{H}}$ of d-dimensional subspaces defined by $\mathcal{H}$ and is associated with the set $\pi_d^{\mathcal{H}}$ of projectors of trace d commuting with $\mathcal{H}$:

$$\pi_d^{\mathcal{H}} = \{\pi, \quad [\pi, \mathcal{H}] = 0 \quad \mathrm{Tr}(\pi) = d\}. \tag{7}$$

In general, the constraints induced by the relations (4)–(7) are not sufficient to define all the entries of the π matrices. The number of remaining independent parameters in π is the dimension of the stratum. This number can be *a priori* determined by group symmetry arguments as developed by Ishii [16–18].

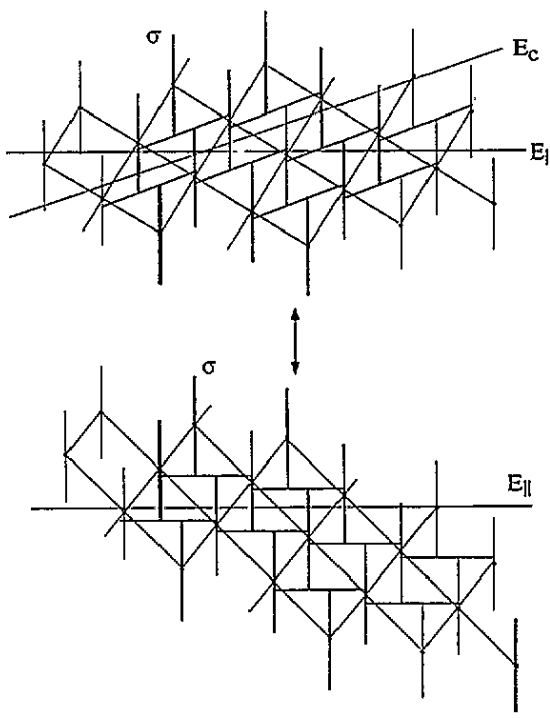

Figure 6. Cutting the atomic surfaces aligned along $\boldsymbol{E}_\perp$ by $\boldsymbol{E}_c$ and projecting onto $\boldsymbol{E}_\parallel$ is equivalent to applying a shear to the hyperlattice that transforms $\boldsymbol{E}_c$ into $\boldsymbol{E}_\parallel$.

3.2. Derivation of the 'shear' method

As mentioned in section 2.1, the shift field cannot be analysed by simple examination of the peak shifts. Since we are interested here only in the geometry of the structure (and the location of the diffraction peaks), we shall assume for simplicity that the atomic surfaces are parallel to $\boldsymbol{E}_\perp$ (i.e. $\boldsymbol{E}_\sigma = \boldsymbol{E}_\perp$). It is clear (see figure 6) according to which description mode—active or passive—is used, that introducing a cut space $\boldsymbol{E}_c$ different from $\boldsymbol{E}_\parallel$ and projecting onto $\boldsymbol{E}_\parallel$ along $\boldsymbol{E}_\perp$ is equivalent to performing a linear *shear* of the lattice Λ along the perpendicular space that transforms $\boldsymbol{E}_c$ into $\boldsymbol{E}_\parallel$. This is the basis of the 'shear' method. In order to explicitly calculate this shear transformation, we define as $M_{\alpha,\beta}$ where $\boldsymbol{E}_\alpha \oplus \boldsymbol{E}_\beta = \mathbb{R}^n$, the $n \times n$ matrices the rows of which are the coordinates of the unit vectors of the subspaces $\boldsymbol{E}_\alpha$ and $\boldsymbol{E}_\beta$ with dimensions respectively d_α and $d_\beta = n - d_\alpha$. For example, the matrix $M_{\parallel,\perp}$ in the icosahedral case ($n = 6$; $d_\parallel = d_\perp = 3$) is defined by

$$M_{\parallel,\perp} = \begin{pmatrix} \mathcal{B}_\parallel \\ \mathcal{B}_\perp \end{pmatrix} = \begin{pmatrix} e^\parallel_{1,1} & e^\parallel_{2,1} & \cdots & e^\parallel_{6,1} \\ e^\parallel_{1,2} & e^\parallel_{2,2} & \cdots & e^\parallel_{6,2} \\ e^\parallel_{1,3} & e^\parallel_{2,3} & \cdots & e^\parallel_{6,3} \\ e^\perp_{1,1} & e^\perp_{2,1} & \cdots & e^\perp_{6,1} \\ e^\perp_{1,2} & e^\perp_{2,2} & \cdots & e^\perp_{6,2} \\ e^\perp_{1,3} & e^\perp_{2,3} & \cdots & e^\perp_{6,3} \end{pmatrix}. \tag{8}$$

These matrices are such that

$$M_{\alpha,\beta}\xi = \begin{pmatrix} \pi_\alpha \xi \\ \pi_\beta \xi \end{pmatrix} = \begin{pmatrix} x^\alpha \\ x^\beta \end{pmatrix} \tag{9}$$

where x^α denote the components of the orthogonal projections along $\boldsymbol{E}_{\alpha^\perp}$ of ξ onto the subspace $\boldsymbol{E}_\alpha$ expressed in the bases $\mathcal{B}_\alpha$ (and similarly for β).

Let ξ be a node of Λ and let ζ be the intersection point of $\boldsymbol{E}_c$ with the affine subspace parallel to $\boldsymbol{E}_\perp$ passing through ξ. The shear transformation from the given quasicrystal to the approximant phase consists in shifting the original vector ξ by $-\pi_\perp \zeta$ as shown in figure 7.

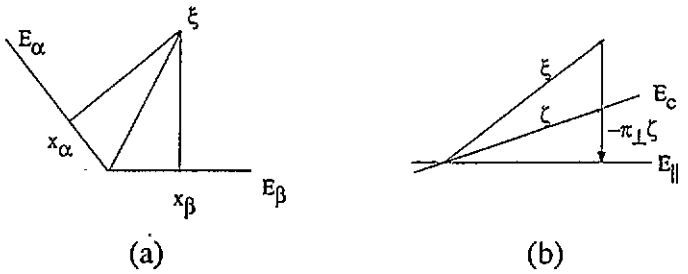

Figure 7. Definition of the variables used to characterize the shear.

The vector ζ is defined by $\pi_{c^\perp}\zeta = 0$ and $\pi_\parallel \zeta = \pi_\parallel \xi$. Thus

$$M_{\parallel,c^\perp}\zeta = \begin{pmatrix} \pi_\parallel \zeta \\ \pi_{c^\perp}\zeta \end{pmatrix} = \begin{pmatrix} \pi_\parallel \xi \\ 0 \end{pmatrix} = M_{\parallel,\perp}\pi_\parallel \xi \tag{10}$$

so that ζ is given by

$$\zeta = M_{\parallel,c^\perp}^{-1} M_{\parallel,\perp} \pi_\parallel \xi \tag{11}$$

and the shear transformation Υ, defined by $\Upsilon \xi = -\pi_\perp \zeta$, can finally be written as

$$\Upsilon = -\pi_\perp M_{\parallel,c^\perp}^{-1} M_{\parallel,\perp} \pi_\parallel. \tag{12}$$

As expected, Υ reduces to zero when the cut space $\boldsymbol{E}_c$ is parallel to the physical space $\boldsymbol{E}_\parallel$.

Now, expressing Υ in the basis $\{\mathcal{B}_\parallel, \mathcal{B}_\perp\}$, we obtain

$$\Upsilon_{\parallel,\perp} = -M_{\parallel,\perp} \pi_\perp M_{\parallel,\perp}^{-1} M_{\parallel,\perp} M_{\parallel,c^\perp}^{-1} M_{\parallel,\perp} \pi_\parallel M_{\parallel,\perp}^{-1}. \tag{13}$$

This product of matrices takes a simple form when written with blocks of submatrices. We denote by $[\cdots]_{(d_1 \times d_2)}$ submatrices with d_1 rows and d_2 columns. Let $d_\parallel$ be the dimension of $\boldsymbol{E}_\parallel$ and $\boldsymbol{E}_c$ and $d_\perp = n - d_\parallel$ the dimension of $\boldsymbol{E}_\perp$ and $\boldsymbol{E}_c^\perp$. We first note the trivial forms

$$\begin{aligned} M_{\parallel,\perp} \pi_\parallel M_{\parallel,\perp}^{-1} &= \begin{pmatrix} [I]_{(d_\parallel \times d_\parallel)} & 0 \\ 0 & 0 \end{pmatrix} \\ M_{\parallel,\perp} \pi_\perp M_{\parallel,\perp}^{-1} &= \begin{pmatrix} 0 & 0 \\ 0 & [I]_{(d_\perp \times d_\perp)} \end{pmatrix} \end{aligned} \tag{14}$$

we can easily calculate $M_{\parallel,\perp} M_{\parallel,c^\perp}^{-1}$ using the fact that

$$M_{\parallel,c^\perp}^{-1} = {}^t M_{c,\perp} A \tag{15}$$

with

$$A = \begin{pmatrix} [e_\parallel \cdot e_c]_{(d_\parallel \times d_\parallel)}^{-1} & 0 \\ 0 & [e_\perp \cdot e_{c^\perp}]_{(d_\perp \times d_\perp)}^{-1} \end{pmatrix} \tag{16}$$

and therefore

$$M_{\parallel,\perp} M_{\parallel,c^\perp}^{-1} = \begin{pmatrix} [I]_{(d_\parallel \times d_\parallel)} & 0 \\ \varepsilon_{(d_\perp \times d_\parallel)} & \gamma_{(d_\perp \times d_\perp)} \end{pmatrix} \tag{17}$$

where $\gamma_{(d_\perp \times d_\perp)}$ is some $d_\perp \times d_\perp$ matrix, so that $\Upsilon_{\parallel,\perp}$ takes the simple block form

$$\Upsilon_{\parallel,\perp} = -\begin{pmatrix} 0 & 0 \\ \varepsilon_{(d_\perp \times d_\parallel)} & 0 \end{pmatrix} \tag{18}$$

where ε is a $d_\perp \times d_\parallel$ matrix given by

$$\varepsilon = [e_\perp \cdot e_c]_{(d_\perp \times d_\parallel)} [e_\parallel \cdot e_c]_{(d_\parallel \times d_\parallel)}^{-1}. \tag{19}$$

As expected, the shear matrix ε is a rectangular matrix $d_\parallel \times d_\perp$ because it relates components in one space ($\boldsymbol{E}_\parallel$) to components in the other space ($\boldsymbol{E}_\perp$).

Expressed in the $\{\mathcal{B}_\parallel, \mathcal{B}_\perp\}$ basis, a hyperlattice node $\xi = \{x_\parallel, x_\perp\}$ transforms under the shear into $\{x'_\parallel, x'_\perp\}$ by the well known relations [21, 23]

$$\begin{aligned} x'_\parallel &= x_\parallel \\ x'_\perp &= x_\perp - \varepsilon\, x_\parallel \end{aligned} \tag{20}$$

which, by Fourier transform, translates into

$$\begin{aligned} q'_\parallel &= q_\parallel + {}^t\varepsilon\, q_\perp \\ q'_\perp &= q_\perp. \end{aligned} \tag{21}$$

The equation (19) shows that the explicit calculation of ε is easily obtained by constructing the two matrices of scalar products of the unit vectors of $\boldsymbol{E}_c$ with those of $\boldsymbol{E}_\parallel$ and $\boldsymbol{E}_\perp$, then inverting the square matrix $[e_\parallel \cdot e_c]_{(d_\parallel \times d_\parallel)}$ and finally performing the left product with $[e_\perp \cdot e_c]_{(d_\perp \times d_\parallel)}$. As already mentioned, a basis of $d_\parallel$ unit vectors of $\boldsymbol{E}_c$ is easily constructed from any $d_\parallel$ columns of the corresponding projector.

To achieve the simplest form in the expression of the shear matrix ε, it is convenient to choose the bases of $\boldsymbol{E}_\parallel$ and $\boldsymbol{E}_\perp$ consistent with the point symmetry of the considered approximant (see appendix B). Let then $R_\parallel$ and $R_\perp$ be two invertible square matrices of rank respectively $d_\parallel$ and $d_\perp$ which relate two bases $\mathcal{B}'_\parallel = R_\parallel \mathcal{B}_\parallel$ and $\mathcal{B}'_\perp = R_\perp \mathcal{B}_\perp$ in respectively $\boldsymbol{E}_\parallel$ and $\boldsymbol{E}_\perp$. The Υ matrix transforms then according to

$$\Upsilon' = -\begin{pmatrix} 0 & 0 \\ \varepsilon' & 0 \end{pmatrix} = -\begin{pmatrix} R_\parallel & 0 \\ 0 & R_\perp \end{pmatrix} \begin{pmatrix} 0 & 0 \\ \varepsilon & 0 \end{pmatrix} \begin{pmatrix} R_\parallel^{-1} & 0 \\ 0 & R_\perp^{-1} \end{pmatrix} \tag{22}$$

which leads to

$$\varepsilon' = R_\parallel\, \varepsilon\, R_\perp^{-1}. \tag{23}$$

This equation shows how ε transforms under changes of bases in either $\boldsymbol{E}_\parallel$ or $\boldsymbol{E}_\perp$. In particular, since the transformation is obviously not a simple conjugation of ε, the trace of ε changes upon changing the bases.

There are cases where the calculation of ε is particularly simple. Indeed, in many practical cases, the experimental data suggest choosing specific lattice vectors of Λ as generators of the unit cell vectors in $\boldsymbol{E}_\parallel$ of the considered approximant. We take the practical example of $d_\parallel = 3$. We designate by $\{a, b, c\}$ the three nodes of Λ which generate the unit vectors of the approximant phase. These three nodes define the cut space $\boldsymbol{E}_c$. They project on $\boldsymbol{E}_\parallel$ and $\boldsymbol{E}_\perp$ as $\{(a_\parallel, a_\perp), (b_\parallel, b_\perp), (c_\parallel, c_\perp)\}$. Equation (19) leads to the following $\varepsilon_{(d_\perp \times 3)}$ matrix:

$$\varepsilon = \begin{pmatrix} a_{\perp,1} & b_{\perp,1} & c_{\perp,1} \\ a_{\perp,2} & b_{\perp,2} & c_{\perp,2} \\ a_{\perp,3} & b_{\perp,3} & c_{\perp,3} \\ \cdots & \cdots & \cdots \\ a_{\perp,d_\perp} & b_{\perp,d_\perp} & c_{\perp,d_\perp} \end{pmatrix} \begin{pmatrix} a_{\parallel,x} & b_{\parallel,x} & c_{\parallel,x} \\ a_{\parallel,y} & b_{\parallel,y} & c_{\parallel,y} \\ a_{\parallel,z} & b_{\parallel,z} & c_{\parallel,z} \end{pmatrix}^{-1}. \tag{24}$$

This simple equation (24) has been successfully used for determining specific cubic, rhombohedral, orthorhombic etc. series of periodic approximants of real quasicrystals (see, for instance, [33, 34]).

4. Periodic approximants

The case of (3D) periodic approximants is of special practical importance. We examine here two basic aspects of these phases in the framework of the 'shear' method just discussed. The first aspect is the characterization of the symmetry of the approximant (space group) as a function of the shear and the second aspect is devoted to the 'degenerate' approximant structures which will be defined later in this section.

4.1. Symmetry of periodic approximants

Although generic approximants of a given $\mathcal{H}$-stratum are quasiperiodic and have no strict point symmetry, their atomic correlations functions are invariant to any order through $\mathcal{H}$. This invariance property is due to the fact that the nodes of the 'sheared' hyperlattice Λ' project onto $E_\perp$ as *uniformly dense 'sheets' of points* which are invariant through $\mathcal{H}$: any two structures obtained by parallel cuts differing only by translations in these dense sheets are locally isomorphic structures [12, 35] and can be viewed as physically equivalent (see for instance [36]). This feature breaks down for periodic approximants: the lattice Λ' projects onto $E_\perp$ as a *discrete set of points* defining a lattice, say $L_\perp$: the possible structures obtained by parallel cuts are either identical (superimposable) or crystallographically different depending on the location of the trace of E_c in $E_\perp$.

To simplify the discussion, we restrict our attention to the simple case where Λ projects uniformly densely onto $E_\perp$ (i.e. we restrict our attention to one local isomorphism class of the parent quasicrystal). Also, we choose a parent quasicrystal which is defined by an unique prototypic atomic surface (the discussion can be trivially extended for structures with several atomic surfaces).

Let us consider a periodic approximant belonging to a given $\mathcal{H}$-stratum where $\mathcal{H}$ is a subgroup of $\mathcal{G}$ obtained by the shear method. As discussed earlier, the initial atomic surface σ with point symmetry $\mathcal{G}$ has been distorted under the shear in order to preserve the overall topology of the parent quasicrystal. We designate by σ' the distorted atomic surface which now has point symmetry $\mathcal{H}$. Projecting the atomic surfaces attached to the lattice nodes of Λ' onto $E_\perp$ is equivalent to copying σ' at each node of $L_\perp$. This projection defines a partition of $E_\perp$ into cells of *finite* volume because $L_\perp$ is a discrete set of points. Also, infinitely many atomic surfaces project in $E_\perp$ exactly on top of each others: they generate translation orbits of equivalent atoms in $E_\parallel$.

The partition in $E_\perp$ being periodic, we can restrict our attention to a single Wigner–Seitz cell of $L_\perp$. We designate by z the trace of E_c in $E_\perp$. The cut space hits the atomic surfaces attached to the lattice nodes of $L_\perp$ which are *inside* a prototypic atomic surface centred on z, which we denote by σ'_z (see figure 8).

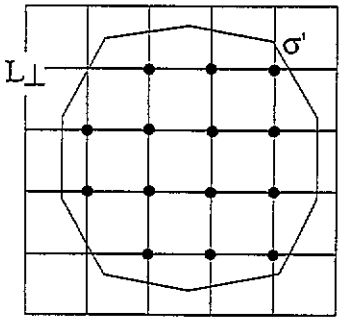

Figure 8. The nodes of $L_\perp$ that project inside σ' in $E_\perp$ define completely the approximant periodic structure; each of these points corresponds to a translation orbit of the real structure.

We call this (finite) set of nodes a 'structure pattern', say $\mathcal{P}_z$:

$$\mathcal{P}_z = \{\xi \in L_\perp; \quad \xi \in \sigma'_z\}. \tag{25}$$

This structure pattern defines the approximant periodic structure. The counting of the possible different structures associated to a given shear field consists in counting the number of cells of the partition inside the Wigner–Seitz cell of $L_\perp$. Each cell is characteristic of a given structure pattern and therefore of a given structure.

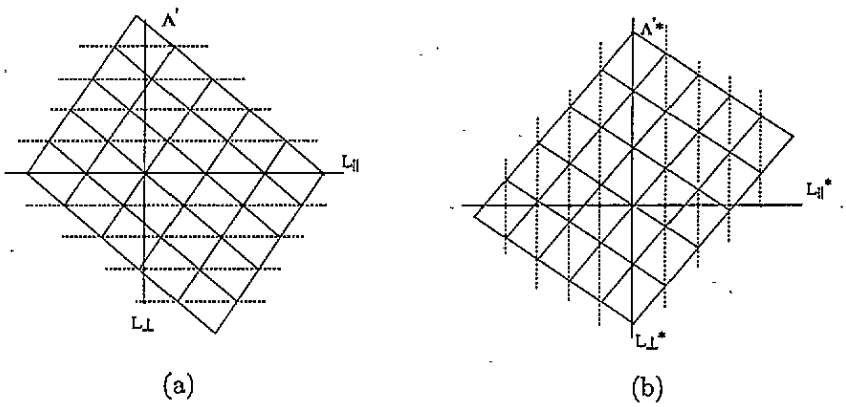

Figure 9. A rational shear of Λ defines sublattices in $E_\parallel$ and $E_\perp$: (*a*) in the direct space the sheared lattice Λ' is such that a sublattice $L_\parallel$ is parallel to $E_\parallel$ and such that the orthogonal projection of Λ' onto $E_\perp$ is a sublattice $L_\perp$; (*b*) in the reciprocal space, $L_\parallel^*$ is the projection onto $E_\parallel^*$ of Λ'^* while $L_\perp^*$ is parallel to $E_\perp^*$.

It is interesting to calculate the Fourier transform of the approximant structure within the standard formalism of quasicrystals. Indeed, owing to the fact that the projection of Λ' onto $E_\perp$ is a lattice ($L_\perp$) and that $E_\parallel$ is parallel to a sublattice of Λ', say $L_\parallel$ (see figure 9), we deduce that the projection of Λ'^* onto $E_\parallel{}^*$ is the (reciprocal) lattice $L_\parallel^*$ and that $E_\perp{}^*$ is parallel to the sublattice $L_\perp^*$ of Λ'^*. The lattices $L_\parallel^*$ and $L_\perp^*$ are the reciprocal lattices of respectively $L_\parallel$ and $L_\perp$. Now, let $q'_\parallel$ be a node of $L_\parallel^*$. The structure form factor $F(q'_\parallel)$ is given by

$$F(q'_\parallel) = \sum_j f_j \exp(2i\pi q'_\parallel \cdot x'_j) \tag{26}$$

where the sum extends over all atomic sites x'_j with atomic species j of form factor f_j inside the unit cell of $L_\parallel$. We observe that $q'_\parallel$ is the projection of a node, say Q', of Λ'^* modulo any translation of $L_\perp^*$. On the other hand, x'_j is the projection of a (unique) node ζ'_j of Λ', which, in turn, projects in $E_\perp$ on a node ξ'_j of $L_\perp$. Since $Q' \cdot \zeta' = k \in \mathbb{Z}$ for every $Q' \in \Lambda'^*$ and $\zeta' \in \Lambda'$, the scalar products $q'_\parallel \cdot x'_j$ can equivalently be written as $-q'_\perp \cdot \xi'_j$ where $q'_\perp$ is the projection on $E_\perp^*$ of Q' modulo $L_\perp^*$ (adding any vector of $L_\perp^*$ to Q' introduces an irrelevant integer value in the scalar product). We can then write the structure factor (26) as:

$$F(q'_\parallel) = \sum_{\xi'_j \in \mathcal{P}_z} f_j \exp(-2i\pi q'_\perp \cdot \xi'_j) \tag{27}$$

where $q'_\perp$ is the projection onto $E^*_\perp$ of an arbitrarily chosen node of the set $Q' + L^*_\perp$. Using relations (20) and (21), we can express the structure factor of the approximant as a function of the parent quasicrystal components $\xi_\parallel$, $\xi_\perp$ and $q_\parallel$, $q_\perp$ and the shear strain ε, as

$$F(q_\parallel + {}^t\varepsilon q_\perp) = \sum_{\xi_\perp - \varepsilon\xi_\parallel \in \sigma'} f_j \exp[-2i\pi q_\perp \cdot (\xi_\perp - \varepsilon\xi_\parallel)]. \tag{28}$$

This formula—which is trivially extended for the case of several atomic surfaces and atomic species—is the 'discrete' version of the standard Fourier transform of the window or acceptance function after a rational shear ε in $E_\perp$. It is very handy for numerical calculations of the structure form factors of approximants when starting from the parent quasicrystal data. Observe that the location z of the trace of E_c in $E_\perp$ appears in (27) only through the definition of the structure pattern in the summation. Hence, any variation in z that does not change $\mathcal{P}_z$, leaves as requested, the structure form factor invariant.

The boundaries of the cells correspond to translations of $L_\perp$ where one or several nodes of the structure pattern are on the boundary of σ'. These cells correspond to the usual 'existence' domains of finite configurations in a quasiperiodic structure, except that, here, each cell corresponds to an infinite periodic substructure.

The relative size of the cells are no longer related to the frequency of the corresponding patterns. If one assumes that all these different periodic structures are thermodynamically equivalent, a possible physical interpretation of these relative sizes, is the following: during the transformation from the parent quasicrystal to crystal, nucleation occurs randomly in the sample corresponding to random location of the trace of E_c into $E_\perp$. Then, the relative sizes of the cells correspond to the volume fractions of the different approximant structures in the bulk specimen after complete transformation. The morphology of the transformed material is an intricate mixture of *several different* crystalline structures: it would exhibit not only orientational 'twins' as in standard group/subgroup transformations but also heterophase boundaries, all with a high degree of coherence. These structures share a common skeleton of sites which is reminiscent of 'merohedral' twins in standard crystallography although they (generally) do not share a common lattice. It would be very interesting to check if the micro-crystalline state(s) [26, 37], often observed in the transition from quasicrystal to crystal, is indeed a mixture of microdomains of different structures and not only a fine intrication of microtwinned crystals of a single phase.

Let us now study the symmetry properties of these structures. The procedure described in the previous sections, based on elementary geometry, is independent of the description of the atomic surfaces; it prescribes what point symmetry the translation group should have but it does not predict the actual symmetry of the periodic approximant. Considering one given cell, we observe the following symmetry properties.

(i) Any two z and z' falling in the same cell defines the same structure.

(ii) Any two z and z' falling in cells differing by a non-zero translation of $L_\perp$ define two identical structures shifted by a (non-primitive) translation in $E_\parallel$.

(iii) Any (point) symmetry operation of $\mathcal{H}$, leaving simultaneously invariant σ' and the cell is a symmetry operation of the structure; it is moreover a pure symmetry element (reducible) since at least one translation orbit of points of the structure is left invariant.

(iv) Any (point) symmetry operation of $\mathcal{H}$, leaving simultaneously invariant σ' and the cell modulo a non-zero translation of $L_\perp$, is also a symmetry operation of the structure; this symmetry operation is not necessarily reducible and can possibly correspond to a glide (or screw) symmetry element of the structure.

From these considerations, we find that, in the generic case, a periodic structure generated by a projector of a $\mathcal{H}$-stratum will have a lower point symmetry than $\mathcal{H}$ although

the lattice itself $L_\parallel$ has indeed $\mathcal{H}$ point symmetry. The actual space group of the structure generated by one given cell in $E_\perp$ is obtained by collecting *the hyperspace symmetry elements of* Λ' *which leave invariant simultaneously* σ' *and the cell modulo any translation of* $L_\perp$.

4.2. Cell decomposition

We now consider the special case of parent quasicrystalline structures which can be described by atomic surfaces obtained by union or intersection of the prototypic atomic surface of the canonical tiling. This case is in practice very important since, so far, all the best known icosahedral and decagonal quasicrystals can indeed be satisfactorily described by atomic surfaces that are union or intersection of the corresponding canonical atomic surfaces.

The atomic surfaces of the parent quasicrystal are bounded by facets parallel to the facets of the projected unit cell of Λ' and are therefore traces of rational hyperplanes of Λ'. The construction of the cells for a periodic structure was first demonstrated by Duneau [38] in the case of a family of square approximants in the octagonal tiling.

Let us translate a given structure pattern along a direction normal to a facet of the atomic surface(s). The structure pattern changes each time some points cross the facet. Two such events differ by a translation equal to the reticular distance of the hyperplane defining the facet. Performing this procedure for every facet of the atomic surface(s), we generate an $L_\perp$*-periodic grid pattern which is composed of all traces in* $E_\perp$ *of the reticular hyperplanes parallel to the facets of the atomic surface(s).* Examination of the Wigner–Seitz cell of this grid pattern leads to an exhaustive counting of the possible periodic structures.

4.3. Example of the octagonal tiling

We exemplify the procedure with the octagonal tiling of the plane. As described in appendix A, the octagonal stratum splits into two different square strata corresponding to the two different orbits of mirrors in $8mm$.

We first consider the stratum $4m_1m_2$ (see [38] and appendix A for details on the corresponding projectors). Periodic approximants are found for $\phi = \frac{1}{2}\arctan(p/2q\sqrt{2})$ where p and q are integers such that $p^2 + 8q^2 = n^2$ with n integer. Let us consider for instance the case $p = 1$, $q = 6$ which leads to a periodic structure with a square lattice in $E_\parallel$ with unit cell $a = 3 + 2\sqrt{2}$. Figure 10 shows the corresponding cell decomposition in $E_\perp$: there is only one generic periodic structure with symmetry m (not square!) represented, of course, by four orientational variants deduced from each other by a $\pi/2$ rotation. This square stratum has the remarkable property that all periodic approximants lead to the same cell decomposition (up to a scaling factor) with an unique generic cell.

Let us turn now to the second square stratum generated by $4m_1'm_2'$. Here again periodic approximants are found for $\phi = \frac{1}{2}(\arctan(p/q) - \pi/4)$ where p and q are integers such that $p^2 + q^2 = n^2$ with n integer. We choose, for example, the case $p = 3$, $q = 4$. The cell decomposition gives a grid pattern built with two identical square lattices rotated with respect to each other: the node (p, q) of the first lattice is superimposed to the node (q, p) of the other one. In this example, we recognize in figure 11 five cells corresponding to five different structures.

Only one of these structures has $4mm$ point symmetry ($p4gm$) as shown in figure 12. The corresponding cell is an octagon centred on the special point $(1/2, 1/2)$ of $L_\perp$. Contrary to the previous case, changing the order of the approximant changes the number of different structures: this number increases with the order of the approximant.

These two examples illustrate the various possible situations encountered in the counting of periodic approximant structures of quasicrystals. In general, a periodic approximant has

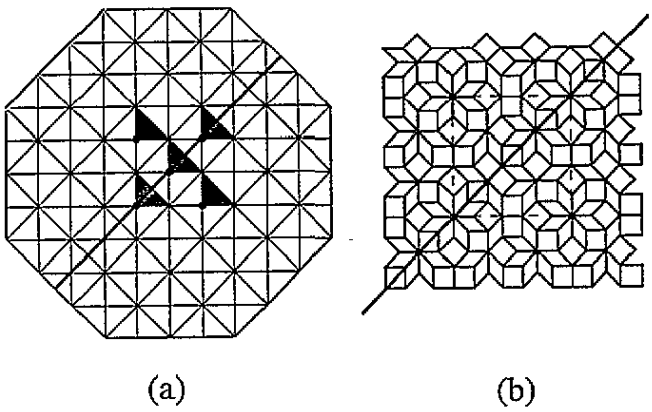

Figure 10. Example of a generic periodic structure of the 'square' stratum $4m_1m_2$: (*a*) the cell decomposition in $E_\perp$ shows an unique cell, the broken region (only a few cells are represented here), which has only a (pure) mirror symmetry as shown on (*b*); the structure has space group *cm*.

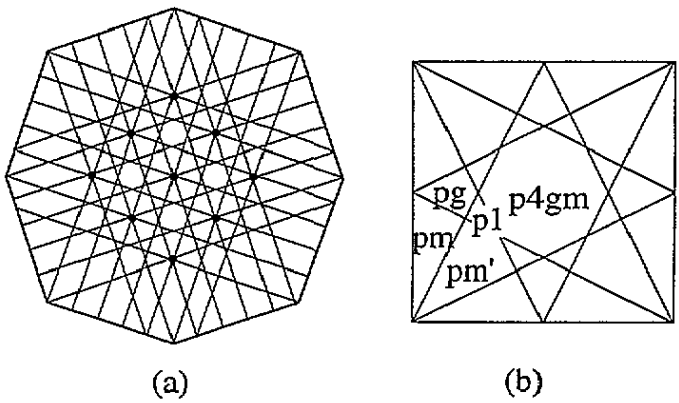

Figure 11. Generic periodic structures of the 'square' stratum $4m_1'm_2'$: (*a*) the cell decomposition in $E_\perp$ shows five cells (irrespective of orientational variants), corresponding to five different structures as shown in (*b*). Observe that, here, non-symmorphic space groups are obtained. Only one of these five structures, whose cell is an octagon centred at the centre of the unit square, has point group *4mm*.

a strictly lower point symmetry than its lattice. The full symmetry is recovered only around some special points of $L_\perp$ (like $(1/2, 1/2)$ in the previous example). In many cases, as illustrated by the $4m_1m_2$ stratum, these special points are located at the intersections of cell boundaries. They correspond to 'degenerate' periodic structures as will be discussed in the next subsection.

4.4. 'Degenerate' periodic structures

An experimental fact is that all presently known approximant structures exhibit a rather high symmetry: the 'cubic' approximants of the ternary systems (Al, Mn, Si) or (Al, Li, Cu) have the largest point group $m\bar{3}$ compatible with the icosahedral group; similarly, diffraction experiments and high resolution imaging of the 'rhombohedral' approximant of the ternary

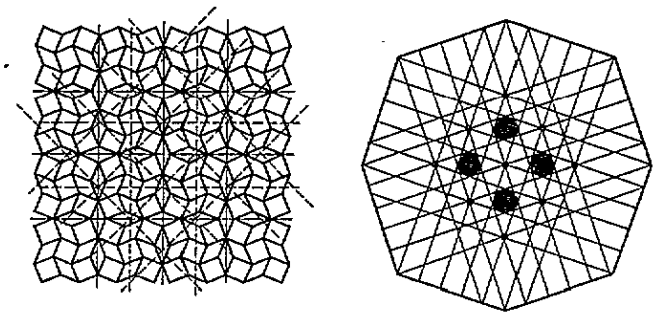

Figure 12. The unique 'square' structure of the stratum $4m'_1m'_2$ with space group $p4gm$ and its corresponding cell (only four such cells, in gray, are drawn for clarity) in $E_\perp$.

system (Al, Cu, Fe) are consistent with the holohedral trigonal symmetry $\bar{3}m$. This suggests that the atomic surfaces of the parent quasicrystal have some particular properties to enforce the cut space to 'lock-in' at some high symmetry points of Λ in order to preserve the highest possible symmetry consistent with the 3D lattice. This, as shown in the preceding subsection, predicts that the special points of $L_\perp$, in the vicinity of which high symmetry periodic approximant are to be found, are privileged locations of the trace of $E_\parallel$. But these are precisely the points where the cell boundaries are most likely to cross: most of these high symmetry periodic approximants would correspond to periodic 'degenerate' structures. We designate these points as 'symmetry dictated lock-in points'.

A plausible explanation of this preferential 'lock-in' is to assume that these high symmetry phases are stabilized through a specific configurational entropy contribution.

Indeed, consider two parallel cuts whose traces in $E_\perp$ fall in two cells adjacent to a common boundary. Passing from one to the other generates a collection of flips for one or several translation orbits of the structures. These two structures share a large number of atomic positions and differ only by those positions, which we call the 'critical flips', whose images in $E_\perp$ are the points of Λ' located at the periphery of σ' and which move in and out of σ'. A substantial increase in configurational entropy can be gained by assuming that these critical flip positions occur with equal probability so that the two structures collapse into one unique average structure which we call a 'degenerate' structure. Since, in this crude picture, we have neglected the possible interactions between critical flips, the average structure mimics a kind of 'local random tiling' model where the atomic flip positions are in one or the other states with equal probability. We can repeat the same process by introducing equal occupation probability to new critical flip sites corresponding to new cell boundaries until we exhaust all the cell boundaries crossing at a single high symmetry point of $L_\perp$. At each step, we proceed to an averaging on a family of critical flips and therefore increase the configurational entropy.

The process is illustrated in figure 13 where the 'square' point symmetry of an octagonal approximant is recovered by averaging the critical flip positions with equal probability.

All approximants of the $\mathcal{H}$-stratum can be seen as ordered decorations of these high symmetry degenerate phases; they share a skeleton of 'stable' points and differ only in the choice of ordering one or several families of critical flips, as exemplified in figure 14 for the case of the square stratum $4m_1m_2$ of the octagonal tiling (the critical flips positions in this case have occupancy numbers 1/2 or 3/8 according to their corresponding locations (edge or vertex) in $E_\perp$).

This leads us to propose the following conjecture: *the 'thermally averaged' periodic structures obtained after a given perpendicular shear of Λ characterizing the phase transition*

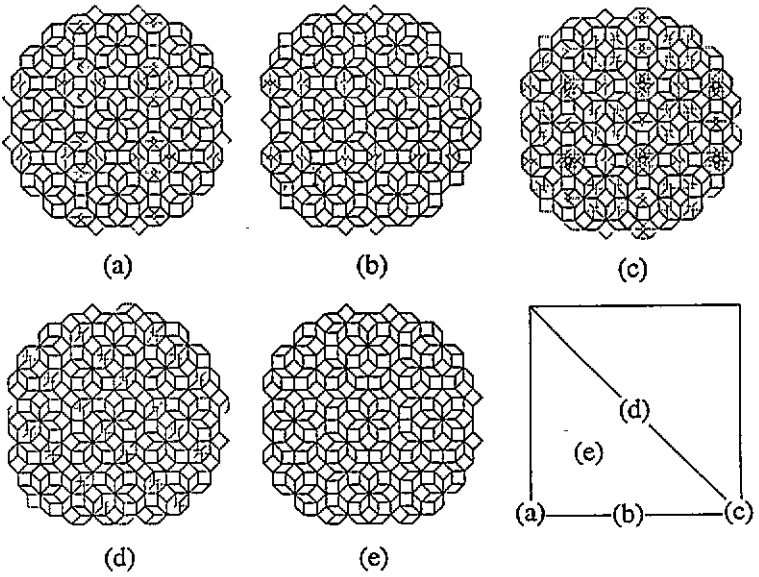

Figure 13. The complete family of periodic approximants belonging to the square symmetry $4m_1m_2$: there are five different structures (irrespective of orientational variants) labelled from (*a*) to (*e*), and their corresponding lock-in points in $E_\perp$. The critical flip positions are drawn with light broken lines. The square symmetry is recovered only at the two special points (0, 0) (structure (*a*)) and (1/2, 1/2) (structure (*c*)) of the elementary domain of $L_\perp$.

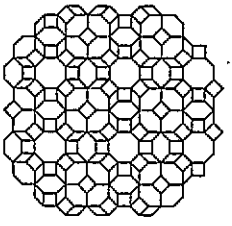

Figure 14. Structures (*b*), (*c*), (*d*) and (*e*) (and variants) of figure 13 share a same skeleton of 'stable' atoms with square symmetry.

from quasicrystal to crystal, are those that maximize the number of nodes of Λ' *projecting on the vertices, the edges and the facets on the atomic surfaces* σ' *in* $E_\perp$. This conjecture is indeed very natural in the context of quasicrystals where atom flips contribute to the entropy of the structure. What we add here, is that another good way to maximize entropy for approximants within a given point symmetry stratum is to 'lock-in' the physical space at some particular points of $E_\perp$. These approximants are periodic only in average; a well defined fraction of their atomic sites (Wyckoff positions) should have fractional occupancy factors when described in a mean-field type approach. We may expect to be able to directly observe these critical positions in the details of the contrasts of the HREM images [39].

Such a conjecture is so far well supported by the presently known approximants in icosahedral and decagonal phases. For example, there are two major approximants of the icosahedral phases: a cubic $m\bar{3}$ phase (α-phase in the (Al, Mn, Si) system and R-phase in the (Al, Li, Cu) system) and a rhombohedral $\bar{3}m$ phase (in (Al, Cu, Fe) system). Assuming that these icosahedral structures can be described by atomic surfaces bounded by twofold planes in $E_\perp$, we arrive at the conclusion that these high symmetry approximant phases should

correspond to 'degenerate' structures with some of their atomic positions being only partially occupied in average, corresponding to a cut located in $E_\perp$ at one of the 'symmetry dictated lock-in points' of $L_\perp$. After the transition is completed at high temperature, successive collective ordering in the critical flip planes (or worms) may appear during the cooling, leading possibly to a microcrystalline morphology. An interesting side effect of this scheme is that periodic approximants would be as good candidates as quasicrystals for studying atom flip dynamics.

Acknowledgments

We are very pleased to thank Drs P Kalugin, F Gähler, M Audier and M Duneau for helpful discussions. We specially thank Dr M Audier who showed us, prior to publication, very intriguing HREM images of an approximant in the (Al, Pd, Mn) system where specific regions in the unit could be explained by columns of critical atom flips. We are very grateful to Professor J W Cahn for his critical and patient review of the manuscript.

Appendix A. Approximants in octagonal tiling

The octagonal tiling can be generated from a simple lattice in a 4D space. It is an excellent example for illustrating the projector technique described in the body of the paper. Here, we will start from the 'ideal' octagonal tiling and derive the strata corresponding to square and rectangle symmetries. We restrict our attention to projectors with trace 2.

It is easily seen that the high symmetry point group $8mm$ contains two (non-conjugate) square groups, say $4m_1m_2$ and $4m_1'm_2'$, each in turn generating two rectangle groups, respectively $\{m_1, m_2\}$ and $\{m_1', m_2'\}$. The point group $8mm$ is generated by the two reflections m_1 and m_1' defined by

$$m_1 = \begin{pmatrix} 1 & 0 & 0 & 0 \\ 0 & 0 & 0 & -1 \\ 0 & 0 & -1 & 0 \\ 0 & -1 & 0 & 0 \end{pmatrix} \qquad m_1' = \begin{pmatrix} 0 & 1 & 0 & 0 \\ 1 & 0 & 0 & 0 \\ 0 & 0 & 0 & -1 \\ 0 & 0 & -1 & 0 \end{pmatrix}. \tag{A1}$$

A general orthogonal projector is written as

$$\pi = \begin{pmatrix} a & b & c & d \\ b & e & f & g \\ c & f & h & i \\ d & g & i & j \end{pmatrix} \qquad \text{with} \quad \pi^2 = \pi. \tag{A2}$$

The commutation relations with m_1 and m_1' leads to the projector of the octagonal tiling:

$$\pi_{\text{octo}} = \frac{1}{2}\begin{pmatrix} 1 & a & 0 & -a \\ a & 1 & a & 0 \\ 0 & a & 1 & a \\ -a & 0 & a & 1 \end{pmatrix} \qquad \text{with} \quad a = \frac{1}{\sqrt{2}} = \cos\frac{\pi}{4}. \tag{A3}$$

A1. Tilings with square symmetry

There are two types of tilings with square symmetry, depending on which subset of mirrors ($\{m_1, m_2\}$ or $\{m'_1, m'_2\}$) is retained. Both subsets correspond to projectors with one free parameter (noted here φ). The first subset (associated to the point group $4m_1m_2$) is characterized by the generic projector

$$\pi_{m_1m_2} = \frac{1}{2}\begin{pmatrix} 1+a & b & 0 & -b \\ b & 1-a & b & 0 \\ 0 & b & 1+a & b \\ -b & 0 & b & 1-a \end{pmatrix} \quad \text{with} \quad \begin{cases} a = \sin 2\varphi \\ b = \frac{1}{\sqrt{2}}\cos 2\varphi \end{cases} \tag{A4}$$

whereas the second subset corresponds to the projector

$$\pi_{m'_1m'_2} = \frac{1}{2}\begin{pmatrix} 1 & a & 0 & -b \\ a & 1 & b & 0 \\ 0 & b & 1 & a \\ -b & 0 & a & 1 \end{pmatrix} \quad \text{with} \quad \begin{cases} a = \cos(2\varphi + \frac{\pi}{4}) \\ b = \sin(2\varphi + \frac{\pi}{4}). \end{cases} \tag{A5}$$

In both cases, the octagonal projector corresponds to $\varphi = 0$. The complementary projector $I - \pi$ is obtained by changing φ into $\varphi + \pi/2$; 2D periodic approximants with lattice parameter a are defined for

$$\begin{aligned} &\text{stratum} \quad m_1m_2 \quad \begin{cases} \varphi = \frac{1}{2}\arctan(p/2q\sqrt{2}) \qquad \text{with} \quad p^2 + 8q^2 = n^2 \\ a = (n + p + 2q\sqrt{2})/\gcd(n + p, q) \end{cases} \\ &\text{stratum} \quad m'_1m'_2 \quad \begin{cases} \varphi = \frac{1}{2}(\arctan(p/q) - \pi/4) \qquad \text{with} \quad p^2 + q^2 = n^2 \\ a = \frac{1}{2}(n - p) + \sqrt{2}q \end{cases} \end{aligned} \tag{A6}$$

where $p, q, n \in \mathbb{Z}$.

A2. Tilings with rectangle symmetry

Each previous family with square symmetry splits into two families of tilings with rectangle symmetry depending on which mirror is retained. These families depend on two free parameters noted φ and θ. Here are the four generic projectors corresponding to each of them.

(i) From $4m_1m_2$:

$$\begin{aligned} \pi_{m_1} &= \frac{1}{2}\begin{pmatrix} 1+a & b & 0 & -b \\ b & 1-c & d & e \\ 0 & d & 1+f & d \\ -b & e & d & 1-c \end{pmatrix} \\ \pi_{m_2} &= \frac{1}{2}\begin{pmatrix} 1+c & b & e & -d \\ b & 1-a & b & 0 \\ e & b & 1+c & d \\ -d & 0 & d & 1-f \end{pmatrix} \end{aligned} \tag{A7}$$

with

$$\begin{aligned} &a = \sin 2\varphi \qquad b = \frac{1}{\sqrt{2}}\cos 2\varphi \qquad c = \frac{1}{2}(\sin 2\varphi + \sin 2\theta) \\ &d = \frac{1}{\sqrt{2}}\cos 2\theta \qquad e = \frac{1}{2}(\sin 2\varphi - \sin 2\theta) \qquad f = \sin 2\theta. \end{aligned} \tag{A8}$$

The square stratum corresponds to $\theta = \varphi$. The octagonal stratum corresponds to $\theta = \varphi = 0$.

(ii) From $4m'_1m'_2$:

$$\pi_{\bar{4}m'_1} = \frac{1}{2}\begin{pmatrix} 1+c & a & -d & -b \\ a & 1+c & b & d \\ -d & b & 1-c & a \\ -b & d & a & 1-c \end{pmatrix}$$
$$\pi_{\bar{4}m'_2} = \frac{1}{2}\begin{pmatrix} 1+d & a & c & -b \\ a & 1-d & b & c \\ c & b & 1-d & a \\ -b & c & a & 1+d \end{pmatrix} \tag{A9}$$

with

$$\begin{aligned} a &= \cos 2\theta \cos(2\varphi + \tfrac{\pi}{4}) & b &= \cos 2\theta \sin(2\varphi + \tfrac{\pi}{4}) \\ c &= \sin 2\theta \sin(2\varphi + \tfrac{\pi}{4}) & d &= \sin 2\theta \cos(2\varphi + \tfrac{\pi}{4}). \end{aligned} \tag{A10}$$

The square stratum corresponds to $\theta = 0$. The octagonal stratum corresponds to $\theta = \varphi = 0$.

Appendix B. Shear matrices for icosahedral quasicrystals

We give in this appendix the general expressions of the ε matrices for the three cases of maximum subgroups $\bar{5}m$, $m\bar{3}$ and $\bar{3}m$ of the $m\bar{3}\bar{5}$ icosahedral group.

B1. Pentagonal stratum

The pentagonal stratum $\bar{5}m$ depends on one continuous parameter φ. The general projector can be written as

$$\pi_{\bar{5}m}(\varphi) = \frac{1}{2\sqrt{5}}\begin{pmatrix} a & b & b & b & b & -b \\ b & c & d & e & d & f \\ b & d & c & d & e & f \\ b & e & d & c & e & g \\ b & d & e & e & c & g \\ -b & f & f & g & g & c \end{pmatrix} \tag{B1}$$

with

$$\begin{aligned} a &= \sqrt{5}(1+\sin 2\varphi) & b &= \cos 2\varphi & c &= (5-\sin 2\varphi)/\sqrt{5} \\ d &= (\sqrt{5}-\sin 2\varphi)/\sqrt{5} & e &= -(\sqrt{5}+\sin 2\varphi)/\sqrt{5} \\ f &= (\sqrt{5}+\sin 2\varphi)/\sqrt{5} & g &= -(\sqrt{5}-\sin 2\varphi)/\sqrt{5}. \end{aligned} \tag{B2}$$

A convenient basis for $E_\parallel$ and $E_\perp$ consists in choosing the x axis along the fivefold direction and the y and z axes along a twofold direction and a mirror perpendicular to this twofold in both spaces:

$$e_x^\parallel = \frac{1}{\sqrt{10}}\{\sqrt{5}, 1, 1, 1, 1, -1\}$$

$$
\begin{aligned}
e_y^{\parallel} &= \frac{1}{\sqrt{2(2+\tau)}}\{0, \tau, 1, -1, 0, \tau\} \\
e_z^{\parallel} &= \frac{1}{\sqrt{10}}\{0, 1-\tau, \tau, \tau, -2, \tau-1\} \\
e_x^{\perp} &= \frac{1}{\sqrt{10}}\{\sqrt{5}, -1, -1, -1, -1, 1\} \\
e_y^{\perp} &= \frac{1}{\sqrt{2(3-\tau)}}\{0, \tau-1, -1, 1, 0, \tau-1\} \\
e_z^{\perp} &= \frac{1}{\sqrt{10}}\{0, \tau, 1-\tau, 1-\tau, -2, -\tau\}.
\end{aligned}
\tag{B3}
$$

In that setting, the cut space E_c is defined by $e_y^c = e_y^{\parallel}$ and $e_z^c = e_z^{\parallel}$ and

$$
e_x^c(\varphi) = \alpha\{\sqrt{5}(1+\sin 2\varphi), \cos 2\varphi, \cos 2\varphi, \cos 2\varphi, \cos 2\varphi, -\cos 2\varphi\} \tag{B4}
$$

with $\alpha = 1/\sqrt{10(1+\sin 2\varphi)}$. The shear matrix ε takes then the simple form

$$
\varepsilon_{\bar{5}m}(\varphi) = \tan\varphi \begin{pmatrix} 1 & 0 & 0 \\ 0 & 0 & 0 \\ 0 & 0 & 0 \end{pmatrix}. \tag{B5}
$$

In the standard setting [40], this matrix transforms by (23) into

$$
\varepsilon_{\bar{5}m}(\varphi) = \tan\varphi/\sqrt{5} \begin{pmatrix} -1 & -\tau & 0 \\ \tau^{-1} & 1 & 0 \\ 0 & 0 & 0 \end{pmatrix}. \tag{B6}
$$

B2. Cubic stratum

The cubic stratum $m\bar{3}$ depends also on a unique continuous parameter φ. The general cubic projector can be written as

$$
\pi_{m\bar{3}}(\varphi) = \frac{1}{2\sqrt{5}} \begin{pmatrix} \sqrt{5} & a & a & b & a & -a \\ a & \sqrt{5} & a & -a & b & a \\ a & a & \sqrt{5} & a & -a & b \\ b & -a & a & \sqrt{5} & -a & -a \\ a & b & -a & -a & \sqrt{5} & -a \\ -a & a & b & -a & -a & \sqrt{5} \end{pmatrix} \tag{B7}
$$

with $a = \cos 2\varphi - \frac{1}{2}\sin 2\varphi$ and $b = \cos 2\varphi + 2\sin 2\varphi$. We choose the cubic bases defined by

$$
\begin{aligned}
&e_x^{\parallel} = n\{1, \tau, 0, -1, \tau, 0\} \qquad e_y^{\parallel} = n\{\tau, 0, 1, \tau, 0, -1\} \qquad e_z^{\parallel} = n\{0, 1, \tau, 0, -1, \tau\} \\
&e_x^{\perp} = n\{-\tau, 1, 0, \tau, 1, 0\} \qquad e_y^{\perp} = n\{1, 0, -\tau, 1, 0, \tau\} \qquad e_z^{\perp} = n\{0, -\tau, 1, 0, \tau, 1\}
\end{aligned}
\tag{B8}
$$

with $n = 1/\sqrt{2(2+\tau)}$.

For the cubic stratum these vectors transform into

$$\begin{aligned} e_x^c &= n_\varphi \{2a, \sqrt{5}+b, 0, -2a, \sqrt{5}+b, 0\} \\ e_y^c &= n_\varphi \{\sqrt{5}+b, 0, 2a, \sqrt{5}+b, 0, -2a\} \\ e_z^c &= n_\varphi \{0, 2a, \sqrt{5}+b, 0, -2a, \sqrt{5}+b\} \end{aligned} \tag{B9}$$

with $n_\varphi = 1/\left(2\sqrt{5+\sqrt{5}\,b}\right)$, from which we derive the shear matrix

$$\varepsilon_{m\bar{3}} = \tan\varphi \begin{pmatrix} 1 & 0 & 0 \\ 0 & 1 & 0 \\ 0 & 0 & 1 \end{pmatrix}. \tag{B10}$$

B3. Trigonal stratum

The trigonal stratum $\bar{3}m$ depends on two continuous parameters φ and θ. The general projector can be written as

$$\pi_{\bar{3}m}(\varphi,\theta) = \frac{1}{2\sqrt{5}} \begin{pmatrix} \sqrt{5}+a & b & b & c & c & d \\ b & \sqrt{5}+a & b & d & c & c \\ b & b & \sqrt{5}+a & c & d & c \\ c & d & c & \sqrt{5}-a & -b & -b \\ c & c & d & -b & \sqrt{5}-a & -b \\ d & c & c & -b & -b & \sqrt{5}-a \end{pmatrix} \tag{B11}$$

where

$$\begin{aligned} a &= \tfrac{1}{3}(2\cos 2\varphi - \sin 2\varphi - 2\cos 2\theta - 4\sin 2\theta) \\ b &= \tfrac{1}{3}(2\cos 2\varphi - \sin 2\varphi + \cos 2\theta + 2\sin 2\theta) \\ c &= \tfrac{1}{3}(\cos 2\varphi + 2\sin 2\varphi + 2\cos 2\theta - \sin 2\theta) \\ d &= \tfrac{1}{3}(\cos 2\varphi + 2\sin 2\varphi - 4\cos 2\theta + 2\sin 2\theta). \end{aligned} \tag{B12}$$

We choose the bases of $E_\parallel$ and $E_\perp$ as a threefold direction of type (1, 1, 1) for x and a twofold direction for y, the z direction being orthogonal to both x and y belongs to a mirror:

$$\begin{aligned} e_x^\parallel &= \frac{1}{\sqrt{6(3+4\tau)}}\{2\tau+1, 2\tau+1, 2\tau+1, 1, 1, 1\} \\ e_y^\parallel &= \frac{1}{\sqrt{2(2+\tau)}}\{-1, 0, 1, 0, -\tau, \tau\} \\ e_z^\parallel &= \frac{1}{\sqrt{6(2+\tau)}}\{1, -2, 1, 2\tau, -\tau, -\tau\} \\ e_x^\perp &= \frac{1}{\sqrt{6(7-4\tau)}}\{2\tau-3, 2\tau-3, 2\tau-3, -1, -1, -1\} \\ e_y^\perp &= \frac{1}{\sqrt{2(3-\tau)}}\{1, 0, -1, 0, 1-\tau, \tau-1\} \\ e_z^\perp &= \frac{1}{\sqrt{6(3-\tau)}}\{-1, 2, -1, 2(\tau-1), 1-\tau, 1-\tau\}. \end{aligned} \tag{B13}$$

For the trigonal stratum these vectors transform into

$$\begin{aligned} e_x^c &= n_\varphi \{\sqrt{5}+t_\varphi, \sqrt{5}+t_\varphi, \sqrt{5}+t_\varphi, u_\varphi, u_\varphi, u_\varphi\} \\ e_y^c &= n_\theta \{-t_\theta, 0, t_\theta, 0, -(\sqrt{5}+u_\theta), \sqrt{5}+u_\theta\} \\ e_z^c &= \frac{n_\theta}{\sqrt{3}} \{t_\theta, -2t_\theta, t_\theta, 2(\sqrt{5}+u_\theta), -(\sqrt{5}+u_\theta), -(\sqrt{5}+u_\theta)\} \end{aligned} \tag{B14}$$

with

$$\begin{aligned} t_\varphi &= 2\cos 2\varphi - \sin 2\varphi \qquad & u_\varphi &= 2\sin 2\varphi + \cos 2\varphi \\ t_\theta &= 2\cos 2\theta - \sin 2\theta \qquad & u_\theta &= 2\sin 2\theta + \cos 2\theta \end{aligned} \tag{B15}$$

and

$$n_\varphi = \left(\sqrt{6(5+\sqrt{5}\,t_\varphi)}\right)^{-1} \qquad n_\theta = \left(2\sqrt{5+\sqrt{5}\,u_\theta}\right)^{-1} \tag{B16}$$

from which we derive the shear matrix

$$\varepsilon_{\bar{3}m}(\varphi,\theta) = \begin{pmatrix} -\tan\varphi & 0 & 0 \\ 0 & \tan\theta & 0 \\ 0 & 0 & \tan\theta \end{pmatrix} \tag{B17}$$

which, in the standard orthogonal bases, leads to

$$\varepsilon_{\bar{3}m} = \frac{1}{6}\begin{pmatrix} a & b & c \\ c & a & b \\ b & c & a \end{pmatrix} \tag{B18}$$

with

$$\begin{aligned} a &= 2\tan\varphi + \tan\theta \\ b &= 2\tan\varphi + (1-3\tau)\tan\theta \\ c &= 2\tan\varphi + (3\tau-2)\tan\theta. \end{aligned} \tag{B19}$$

References

[1] Bancel P A 1991 *Quasicrystals: the State of the Art* ed D P Divincenzo and P J Steinhardt (Singapore: World Scientific) pp 17–55
[2] deWolff P M 1977 *Acta Cryst.* A **33** 493
[3] Janner A and Janssen T 1977 *Phys. Rev.* B **15** 643
[4] Bak P 1985 *Phys. Rev.* B **32** 5764
[5] Bak P *Physica* 1986 **136B&C** 296
[6] Elser V and Henley C L 1985 *Phys. Rev. Lett.* **55** 2883
[7] Henley C L 1985 *J. Non-cryst. Solids* **75** 91
[8] Jaric M V and Mohanty U 1987 *Phys. Rev. Lett.* **58** 230
[9] Duneau M and Katz A 1985 *Phys. Rev. Lett.* **54** 2688
[10] Kalugin P A, Kitayev A Y and Levitov L S 1985 *J. Physique Lett.* **46** L601
[11] Elser V 1985 *Phys. Rev.* B **32** 4892
[12] Katz A and Duneau M 1986 *J. Physique* **47** 181

[13] Elser V 1986 *Acta Cryst.* A **42** 36
[14] Duneau M 1988 *Du Cristal a l'Amorphe* ed C Godreche (Paris: Les Editions de Physique)
[15] Duneau M, Mosseri R and Oguey C 1989 *J. Phys. A: Math. Gen.* **22** 4549
[16] Ishii Y 1989 *Phys. Rev.* B **39** 11862
[17] Ishii Y 1990 *Phil. Mag. Lett.* **62** 393
[18] Ishii Y 1992 *Phys. Rev.* B **45** 5228
[19] Baake M, Joseph D and Kramer P 1991 *J. Phys. A: Math. Gen.* **24** L961
[20] Kramer P, Baake M and Joseph D 1993 *J. Non-Cryst Solids* **153** 650
[21] Yamamoto A and Ishihara K N 1988 *Acta Cryst.* A **44** 707
[22] Yamamoto A 1990 *Quasicrystals (12th Taniguchi Symp.)* ed T Fujiwara and T Ogawa (Berlin: Springer) pp 57–67
[23] Jaric M V and Qiu S-Y 1990 *Quasicrystals (12th Taniguchi Symp.)* ed T Fujiwara and T Ogawa (Berlin: Springer) pp 48–56
[24] Janssen T 1991 *Europhys. Lett.* **14** 131
[25] Gratias D, Cahn J W and Mozer B 1988 *Phys. Rev.* B **38** 1643
[26] Audier M 1990 *Microsc. Microanal. Microstruct.* **1** 405
[27] Audier M and Guyot P 1990 *Third Int. Meeting on Quasicrystals 'Quasicrystals and Incommensurate Structures in Condensed Matter'* ed V C M J Yacaman, D Romeu and A Gomez (Singapore: World Scientific) pp 288–99
[28] Audier M and Guyot P 1990 *Proc. Anniversary Adriatico Research Conf. on Quasicrystals* ed M Jaric and S Lundqvist (Singapore: World Scientific) pp 74–91
[29] Lebail A, Leblanc M and Audier M 1991 *Acta Cryst.* B **47** 451
[30] Leblanc M, Lebail A and Audier M 1991 *Physica* B **173** 329
[31] Kalugin P A 1989 *Europhys. Lett.* **9** 545
[32] Katz A 1992 *From Number Theory to Physics* ed J-M L M Waldschmidt, P Moussa and C Itzykson (Berlin: Springer) pp 496–537
[33] Calvayrac Y *et al* 1990 *J. Chrys. France* **51** 417
[34] Menguy N, Audier M, Guyot P and Vacher M 1993 *Phil. Mag.* B **68** 595
[35] Socolar J E S, Steinhardt P J and Levine D 1985 *Phys. Rev.* B **32** 5547
[36] Mermin N D 1992 *Phys. Rev. Lett.* **68** 1172
[37] Motsch T, Denoyer F, Launois P and Lambert M 1992 *J. Phys. France* **2** 861
[38] Duneau M 1991 *J. Phys. France* **1** 1591
[39] Audier M (private communication) recently obtained high resolution images in approximant phases of AlPdM which indeed seem to support the hypothesis of a systematic distribution of critical atomic positions embedded in a well defined periodic skeleton of atoms.
[40] Cahn J W, Shechtman D and Gratias D 1986 *J. Mat. Res.* **1** 13